Vol. 92: 21–31, 2024
https://doi.org/10.3354/cr01731

CLIMATE RESEARCH
Clim Res

Published January 18

Contribution to CR Special 36 'Observed changes in climate over Asia'

Long-term trend of near-surface air temperature lapse rate over the Chinese mainland during 1961–2018

Yun Qin[1,2], Guoyu Ren[1,2,*], Panfeng Zhang[3], Yunjian Zhan[4], Siqi Zhang[1,2], Xiaoying Xue[1,2]

[1]Laboratory for Climate Studies, National Climate Center, China Meteorological Administration, Beijing 100081, PR China
[2]Department of Atmospheric Science, School of Environmental Studies, China University of Geosciences, Wuhan 430074, PR China
[3]College of Geographical Sciences and Tourism, Jilin Normal University, Siping 136000, PR China
[4]National Meteorological Information Center, China Meteorological Administration, Beijing 100081, PR China

ABSTRACT: The near-surface air temperature lapse rate (SATLR) is a result of surface energy balance, and the long-term trend of SATLR is linked to elevation-dependent warming (EDW). The long-term trend of SATLR in China's mainland was examined in the present study. It was found that the regional average values of annual, autumn, and winter SATLR anomalies in T_{mean}, T_{max}, and T_{min} decreased significantly during the period of 1961–2018. In terms of spatial distribution, most of the annual SATLR trends in T_{mean} across China's mainland are negative. In spring, positive SATLR trends in T_{mean} are widespread in the northern mountainous areas of China, while in winter, strong negative trends are found in some areas of the central and eastern parts of the Tibetan Plateau and the Yunnan-Guizhou Plateau. Most of the negative annual SATLR trends in T_{max} occur in the central part of China, but in the southwestern part of China for T_{min}. Widespread negative SATLR trends in T_{min} are usually found in winter, especially in the Hengduan Mountains of Southwestern China and the eastern part of the Tibetan Plateau. The significant positive SATLR trends in T_{max} are observed in spring, mostly distributed in northern mountainous areas. In the context of global and regional warming, the long-term trend of SATLR has the potential to detect differences in altitude responses to climate change on a small spatial scale, and to explore the local effect of EDW.

KEY WORDS: Temperature lapse rate · Long-term trend · Variation · Elevation-dependent warming · Surface air temperature · China

1. INTRODUCTION

The near-surface air temperature lapse rate, also called surface air temperature lapse rate (SATLR), is a result of land surface energy balance, which is defined as the rate of near-surface air temperature (SAT) decreasing with the increase of altitude (Whiteman 2000, Minder et al. 2010, Hartmann 2016). In order to keep consistent with the definition in the atmospheric science community (Gardner et al. 2009, Minder et al. 2010, X. Li et al. 2013, Y. Li et al. 2015, Shen et al. 2016, He & Wang 2020), we consider a positive SATLR as temperature decreasing with increasing altitude and a negative SATLR as temperature increasing with increasing altitude.

SATLR was characterized by hourly/diurnal variation in the day, monthly/seasonal variation in the year, and interannual to multi-decadal variation. Many previous studies focused on the monthly/seasonal variation (Rolland 2003, Marshall et al. 2007, Blandford et al. 2008, Minder et al. 2010, Kattel et al. 2013, 2018, Li et al. 2015, Shen et al. 2016, Ojha 2017, Du et al. 2018). However, only a few studies discussed the hourly/diurnal variation (Pepin et al.

*Corresponding author: guoyoo@cma.cn

Publisher: Inter-Research · www.int-res.com

1999, Pepin & Kidd 2006, Tang & Fang 2006, Wang et al. 2018) and interannual to multi-decadal variation of SATLR (Pepin 2001, Li et al. 2013, Guo et al. 2016, He & Wang 2020). They were usually taken as a part of the research on spatiotemporal variation of SATLR, although a few studies emphasized the interannual to multi-decadal variation. The long-term trend of SATLR in a certain period, which was sometimes related to the multi-decadal to century-scale variation, is worth examining, as it was also linked to elevation-dependent warming (EDW) (Pepin 2001, Guo et al. 2016), and might play an important role in modulating climate sensitivity to external drivers. According to the above-mentioned definition of SATLR, when high elevations warmed faster than the low, the long-term trend of SATLR was negative, and when the low elevations warmed faster than the high, it was positive.

There are only a few previous studies which have examined the long-term trend of SATLR in China. For instance, Li et al. (2013) found that most of China had increasing trends of annual SATLR except for the southwest part of China and the northern part of Xinjiang Province, and an opposite trend of annual SATLR between the eastern and central parts of the Tibetan Plateau, with SATLR decreasing (i.e. became shallow) in the eastern part and increasing (i.e. became steep) in the central part. However, the spatial resolution they used was too coarse to reflect more details in spatial scale. He & Wang (2020) also detected an increasing trend in the country-wide average of annual SATLR. However, they were focused more on the differences in the long-term trends between the SATLR and the land surface temperature lapse rate, than on the distribution characteristics of the long-term trends. Few studies have paid much attention to long-term SATLR. Therefore, to make up for the gap, we focused on researching the long-term trend of SATLR in China. In this article, the research goal is to reveal the characteristics of long-term changes in SATLR in China's mainland, including the spatiotemporal distribution of long-term SATLR trends over 1961–2018 and the changing trend of regional averaged SATLR anomalies, applying a dataset of >2400 meteorological stations.

2. MATERIALS AND METHODS

2.1. Data

The data on the monthly mean, maximum, and minimum of SAT (T_{mean}, T_{max}, and T_{min}) and the altitudes of stations were provided by the National Meteorological Information Center (NMIC), China Meteorological Administration. Quality control and homogeneity adjustment had already been made by NMIC (Cao et al. 2016). There was a total of 2419 meteorological stations in the dataset, the spatial distribution of which was characterized as dense in the east part of China and sparse in the west. The topography of the study area (China's mainland) and the information on geographical position are shown in Fig. 1.

The time period of 1961–2018 was used. There were no missing values in the records of altitudes of stations, and the altitudes ranged from −47.4 to 4801.2 m. The missing data of the SAT were replaced by the values predicted by a recurrent neural network (RNN) algorithm, the program codes of which were obtained from GitHub (Atabay 2016). The low root mean squared error between the predicted values calculated by the RNN algorithm and the observed values in the monthly SAT series indicated that the imputation method for missing data was reasonable (Qin et al. 2021a). The annual/seasonal mean (spring: March, April, May; summer: June, July, August; autumn: September, October, November; winter: December, January, February) of T_{mean}, T_{max}, and T_{min} at each station were then calculated.

2.2. Estimation of SATLR

Due to the limitation of simple linear regression and moving window regression methods, which were frequently used in previous studies, a geographically weighted regression (GWR) model was applied to estimate the annual/seasonal mean SATLR in this research, which was more reasonable for a large region with complex terrain and climatic conditions (Brunsdon et al. 1996, Fotheringham et al. 2002, Fischer & Getis 2010). In the GWR model, the annual/seasonal mean SATLR at each station was estimated by the weighted linear relationship between the annual/seasonal mean of SAT and the altitudes of its surrounding stations within the adaptive bandwidth size, which was defined as the distance of the 17^{th} nearest neighbor station (Qin et al. 2021b). Small bandwidth had the ability to reveal the spatial pattern of SATLR on a small spatial scale, e.g. a small mountainous area, while large bandwidth could present the spatial variation of SATLR on a large spatial scale, e.g. a large plateau area (Fotheringham et al. 2002, Lu et al. 2017).

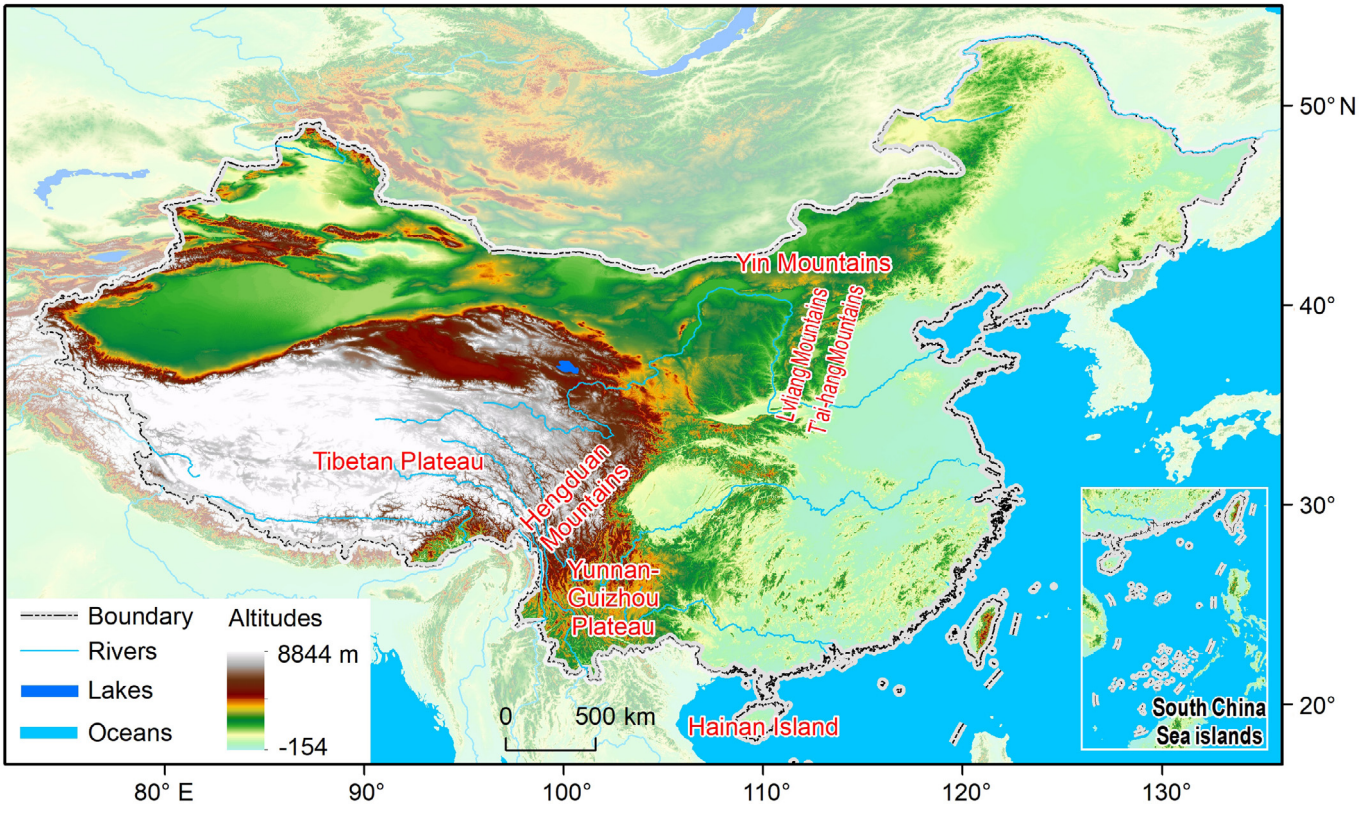

Fig. 1. Topography of the study area

The regression coefficient for the altitude in the GWR model with the local R^2 (i.e. a measure of goodness of fit) <0.7 or the condition number >30 was considered as an invalid SATLR (Mitchell 2005, ESRI 2018, Qin et al. 2021b). Consequently, there were some stations where the values of annual/seasonal mean SATLR series in some years were missing, especially in the flat areas with little altitude variation, which could induce uncertainties. In order to reduce the uncertainties, for each annual/seasonal mean SATLR series, if the number of missing values was >5, the series was removed. For the remaining series, the criteria for judging SATLR were broadened until there were no missing values. After that, a few series with negative SATLR (i.e. temperature inversion) were removed, and then all of the SATLR values in the research were positive.

Finally, there were 916, 793, 1037, 845, and 446 stations in the annual, spring, summer, autumn, and winter SATLR series of T_{mean}, respectively; 867, 769, 908, 824, and 464 stations in the annual, spring, summer, autumn, and winter SATLR series of T_{max}, respectively; and 575, 506, 784, 511, and 299 stations in the annual, spring, summer, autumn, and winter SATLR series of T_{min}, respectively.

2.3. Regional averaging and trend analysis

Firstly, in order to overcome the problem that could be caused by the sparse coverage in some areas, the annual/seasonal mean SATLR anomalies (hereinafter shortened to SATLR anomalies) with respect to the reference period of 1961–1990 were calculated (Jones & Hulme 1996). Secondly, the SATLR anomalies of all available stations in each grid box (1° latitude × 1° longitude) were merged into one SATLR anomaly with the arithmetic average method, due to the low standard deviation of SATLR in the grid box. Thirdly, the regional average SATLR anomalies were calculated with the grid box area-weighted average method, and the cosine of the center latitude of each available grid box was set as the weight (Jones & Hulme 1996). Note that the regional average value was actually the average in the mountainous areas of China's mainland, where the estimate of the SATLR was valid. Finally, as the SATLR anomalies might not have a Gaussian distribution and they were almost correlated in time (von Storch & Navarra 1999), the long-term trends for each available grid box and the regional average SATLR anomalies were estimated with a modified Theil-Sen estimator that diminished

the effect of lag-1 autocorrelation using an iterative pre-whitening process (Sen 1968, Zhang et al. 2000, Wang & Swail 2001). The significance of trends was tested with a Mann-Kendall test (Mann 1945, Kendall 1957, Hirsch et al. 1982). Details of this method to estimate the trends were given by Wang & Swail (2001). In addition, the change points of regional average annual/seasonal mean SATLR anomalies detected with the Mann-Kendall method occurred mostly between 1982 and 1986. For the convenience of comparison, the year of 1984 was used to divide the time periods, and then the trend over 1961–1984 and 1984–2018 were calculated respectively with the above-mentioned method.

If the SATLR trend was significantly negative, it indicated that the value decreased over the time period, and the SATLR became shallow; if the SATLR trend was significantly positive, it indicated that the value increased over the time period, and the SATLR became steep. To better understand this, 2 cases were used to expound the change in SATLR. One showed a negative/decreasing change in SATLR from the early period (1961–1980) to the late period (1999–2018), which was exemplified by the winter mean SATLR in T_{mean} at Xinlong Station located in the Hengduan Mountains (Fig. 2a); the other showed a positive/increasing change in SATLR, exemplified by the spring mean SATLR in T_{mean} at Jiexiu Station located in the T'ai-hang Mountains (Fig. 2b). As shown in Fig. 2, all stations underwent warming; however, the warming amplitudes were different between high altitudes and low altitudes, which resulted in the change in SATLR at the center station. In the first case, the high altitudes warmed faster than the low ones, and SATLR decreased from 6.4 to 5.6°C km^{-1} (Fig. 2a), which indicated that there was a negative SATLR trend over time. Contrarily, the low altitudes warmed faster than the high altitudes in the second case, and SATLR increased from 5.2 to 5.9°C km^{-1} (Fig. 2b), which indicated a positive SATLR trend.

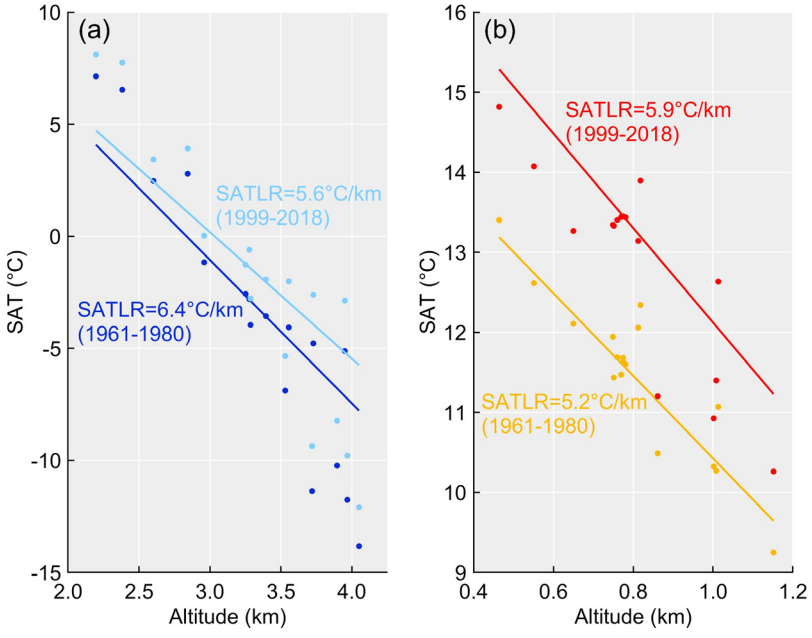

Fig. 2. Scatter of altitude and near-surface air temperature (SAT) at the 17 nearest neighbor stations to (a) Xinlong Station (an example of negative/decreasing change of near-surface air temperature lapse rate [SATLR]) and (b) Jiexiu Station (an example of positive/increasing change of SATLR). The slope represents the SATLR estimated with the geographically weighted regression (GWR) model. Note the different *x*- and *y*-axis scales between (a) and (b)

3. RESULTS

3.1. SATLR trends in T_{mean} (Figs. 3 & 4)

The regional average annual SATLR anomalies in T_{mean} showed a significant (at the 5% level) decreasing trend of −0.028°C km^{-1} decade^{-1} during the period of 1961–2018 (Table 1, Fig. 3b). Most of the annual SATLR trends across China's mainland were negative, with lower than −0.1°C km^{-1} decade^{-1} in the Hengduan Mountains and the eastern part of Tibetan Plateau (Fig. 3a).

In terms of the seasonal SATLR in T_{mean}, the regional average SATLR anomalies had significant decreasing trends over 1961–2018 in summer, autumn, and winter, but not in spring (Table 1, Fig. 4). Positive trends were frequently observed in northern mountainous areas in spring, with larger trends in the Yin Mountains, the T'ai-hang Mountains, and the Lvliang Mountains (Fig. 4a). Although the number of grid cells with SATLR values was relatively low in winter than in the other seasons, strong decreasing trends (<−0.2°C km^{-1} decade^{-1}) were found in some areas of the central and eastern parts of the Tibetan Plateau and the Yunnan-Guizhou Plateau (Fig. 4d).

In the earlier period of 1961–1984, the regional average SATLR anomalies in T_{mean} showed significant decreasing trends in summer (Table 1, Fig. 4b), and the later period of 1984–2018 underwent significant decrease in winter (Table 1, Fig. 4d).

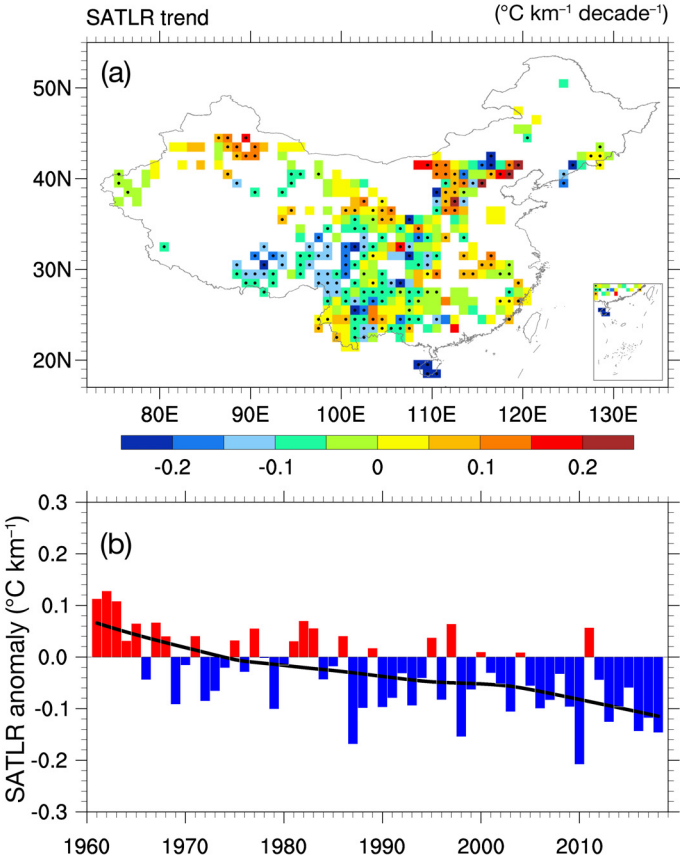

Fig. 3. (a) Trend distribution of grid-box annual near-surface air temperature lapse rate (SATLR) anomalies and (b) regional average annual SATLR anomalies in T_{mean}. Grids with statistically significant (at the 5% level) trends are stippled. The black smooth curve in (b) was achieved with a locally weighted scatter smoothing method (Cleveland 1979)

3.2. SATLR trends in T_{max} and T_{min} (Figs. 5–7)

The regional average annual SATLR anomalies both in T_{max} and T_{min} showed significant decreasing trends over 1961–2018, with −0.030 and −0.027°C km^{-1} decade^{-1}, respectively (Table 1, Fig. 5c,d). Although the direction of regional average trends was the same and the values were close, the spatial distribution was different; many negative SATLR trends in T_{max} occurred in the central part of China, but in the southwestern part of China for T_{min} (Fig. 5a,b).

The regional average values of summer, autumn, and winter SATLR anomalies in T_{max} and those of autumn and winter SATLR anomalies in T_{min} showed significant decreasing trends over 1961–2018 (Table 1, Figs. 6 & 7).

In spring, though the regional average trend of SATLR anomalies in T_{min} was not statistically significant, widespread positive trends were found in some parts of northern and northwestern China (Fig. 6a). In winter, there were strong and widespread negative SATLR trends in T_{min} (<−0.2°C km^{-1} decade^{-1}), with a regional average value of −0.123°C km^{-1} decade^{-1} (Table 1, Fig. 7d).

In the earlier period of 1961–1984, the regional average SATLR anomalies in T_{max} underwent significant decreasing trends in summer, with −0.078°C km^{-1} decade^{-1} (Table 1, Fig. 6b). For the regional average SATLR anomalies in T_{min}, the strong significant decreasing trends occurred in winter over the later period of 1984–2018, with a value of −0.147°C km^{-1} decade^{-1} (Table 1, Fig. 7d).

4. DISCUSSION

The estimation of SATLR should be treated with caution where the linear relationship between altitude and SAT was not perfect. In this article, we utilized the GWR model to estimate SATLR, which was proved to be reasonable for the annual/seasonal mean series (Qin et al. 2021b). However, to avoid the missing values introduced through the process of judgement for SATLR, we broadened the judgement criteria, which could result in error. In addition, the missing values of SAT may have also induced uncertainty, as the filled values might be different from the true values.

The regional average annual SATLR anomalies in T_{mean}, T_{max}, and T_{min} showed a significant decreasing trend during the period 1961–2018 (Table 1, Figs. 3b & 5c,d). This indicated that the SATLR became shallow in most of the mountainous areas of China's

Table 1. Trends in regional average annual/seasonal near-surface air temperature lapse rate (SATLR) anomalies (°C km^{-1} decade^{-1}). Statistically significant (at the 5% level) trends shown in **bold**

SATLR anomalies	Period	Annual	Spring	Summer	Autumn	Winter
T_{mean}	1961–2018	**−0.028**	−0.004	**−0.033**	**−0.035**	**−0.075**
	1961–1984	−0.025	−0.004	**−0.056**	−0.058	−0.040
	1984–2018	−0.020	0.005	−0.011	−0.031	**−0.079**
T_{max}	1961–2018	**−0.030**	0.010	**−0.043**	**−0.036**	**−0.045**
	1961–1984	−0.025	0.028	**−0.078**	−0.045	0.032
	1984–2018	−0.007	0.022	−0.019	−0.014	−0.020
T_{min}	1961–2018	**−0.027**	−0.004	−0.009	**−0.037**	**−0.123**
	1961–1984	−0.009	0.003	−0.005	−0.001	−0.054
	1984–2018	**−0.029**	0.014	−0.003	−0.041	**−0.147**

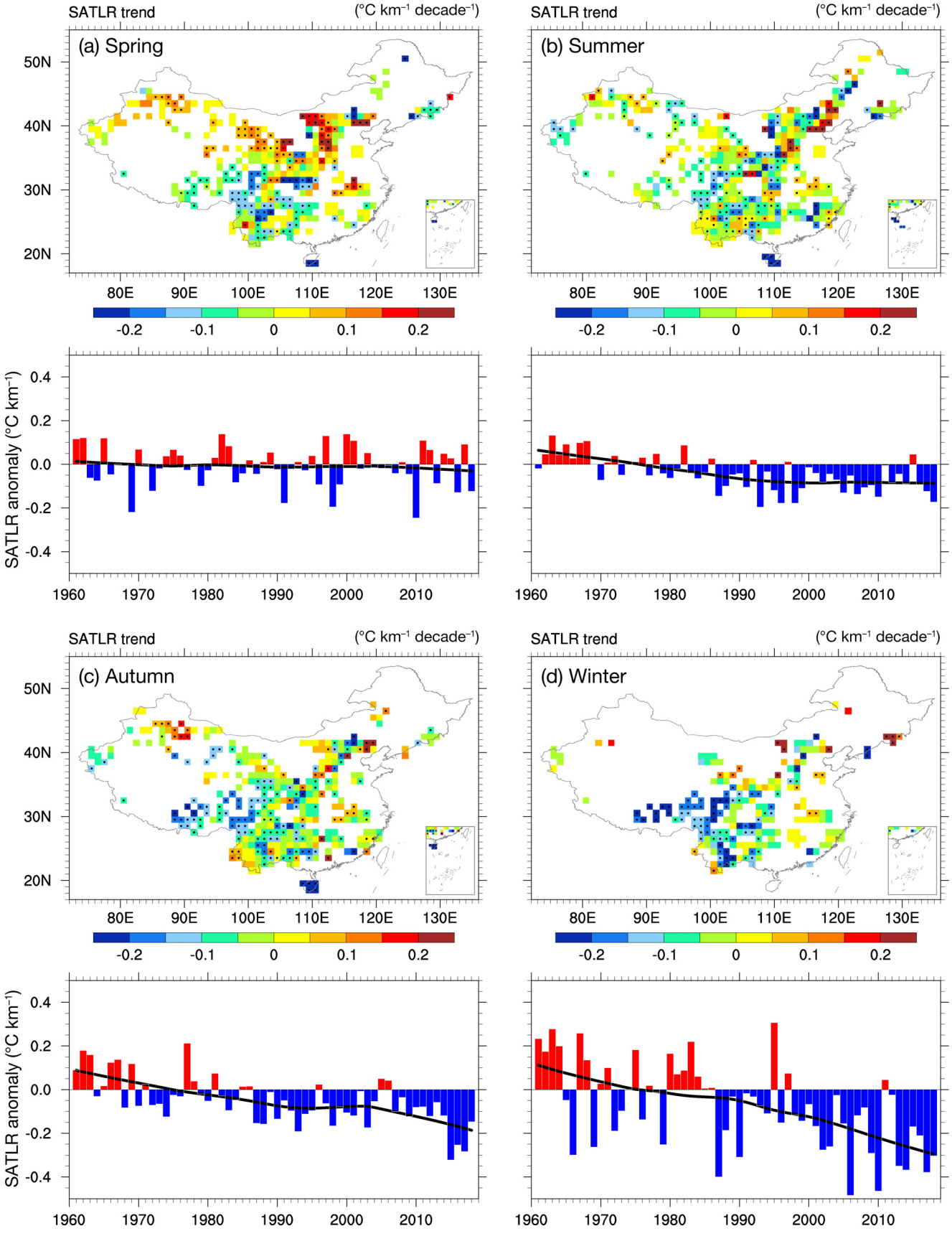

Fig. 4. Trend distribution of grid-box seasonal near-surface air temperature lapse rate (SATLR) anomalies and regional average seasonal SATLR anomalies in T_{mean} for (a) spring, (b) summer, (c) autumn, and (d) winter. Other details as in Fig. 3

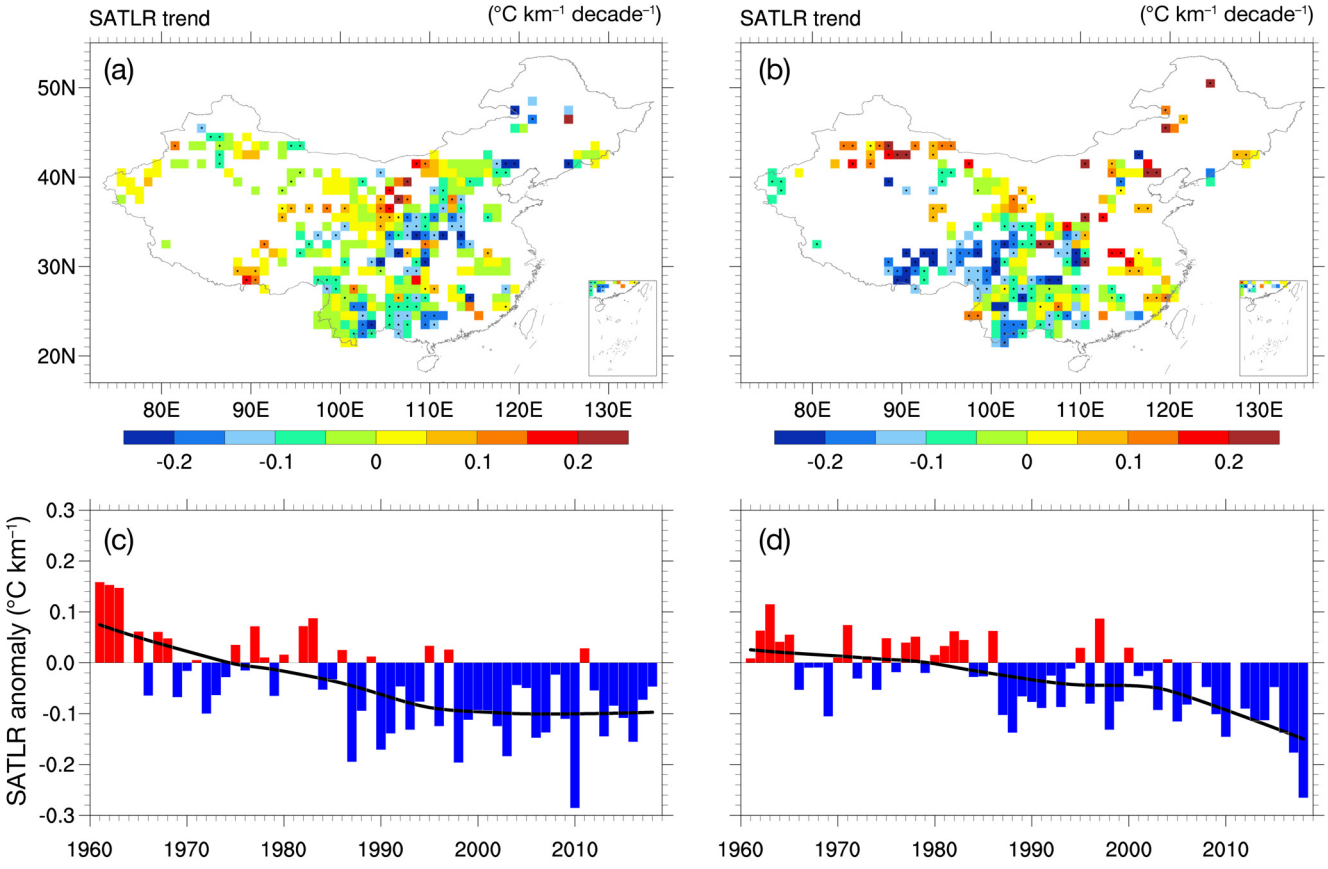

Fig. 5. Trend distribution of grid-box annual near-surface air temperature lapse rate (SATLR) anomalies in (a) T_{max} and (b) T_{min} and regional average annual SATLR anomalies in (c) T_{max} and (d) T_{min}. Other details as in Fig. 3

mainland. The result was opposite to that of Li et al. (2013), who showed an overall increasing trend in the whole of China's mainland. The difference may have been caused by the different coverage of the study area; the regional average SATLR in this article represented only the value in the mountainous areas, not the whole of China's mainland. Nevertheless, the decreasing SATLR trend in the eastern part of the Tibetan Plateau was accordant in the 2 studies.

The phenomenon that negative SATLR trends in T_{max} occurred mainly in the central part of China, but in the southwestern part of China for T_{min}, might be caused by the difference of SATLR sensitivity between T_{max} and T_{min} to the variation of climatic variables (Fig. 5a,b). The SATLR trend could be related to the variation of soil water, specific humidity, cloud cover, and albedo, and these mechanisms are comprehensive and complex (Mountain Research t EDW Working Group 2015). It will be necessary to make further analyses in the future.

According to the definition of SATLR, when the SATLR became shallow, it indicated that the high elevations warmed faster than the low elevations (Fig. 2a), i.e. positive EDW; when it became steep, the low elevations warmed faster than the high ones (Fig. 2b), i.e. negative EDW. The relationship between the negative SATLR trend and the positive EDW was proved with the observed data in the Tibetan Plateau by Guo et al. (2016). In addition, as the intensity of EDW was probably spatially heterogeneous on a large scale of mountainous areas, it was not a simple linear relationship between altitudes and warming rates (Pepin & Seidel 2005, Pepin & Lundquist 2008, You et al. 2010). Not only the intensity, but also the direction of EDW was probably not consistent. For instance, Wang et al. (2014) detected positive EDW in the southern part of the Tibetan Plateau, but negative EDW in the northern part. The SATLR trend has the ability to measure the difference in the warming rate between the 2 altitudes by 1 km vertical distance in the context of warming, which could probably be used to detect differences in altitude response to climate change on a small spatial scale, and to examine the local effect of EDW.

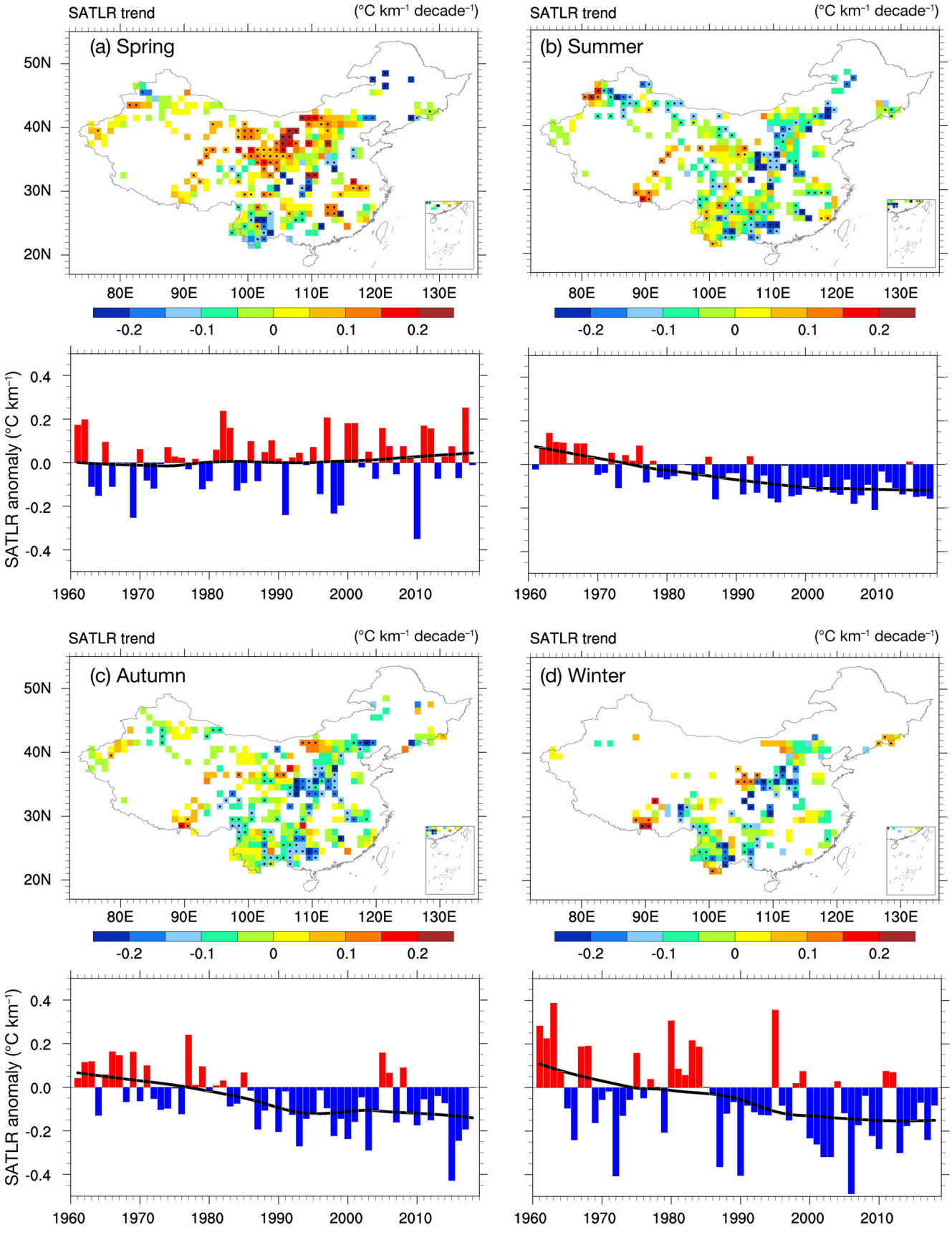

Fig. 6. Trend distribution of grid-box seasonal near-surface air temperature lapse rate (SATLR) anomalies and regional average seasonal SATLR anomalies in T_{max} for (a) spring, (b) summer, (c) autumn, and (d) winter. Other details as in Fig. 3

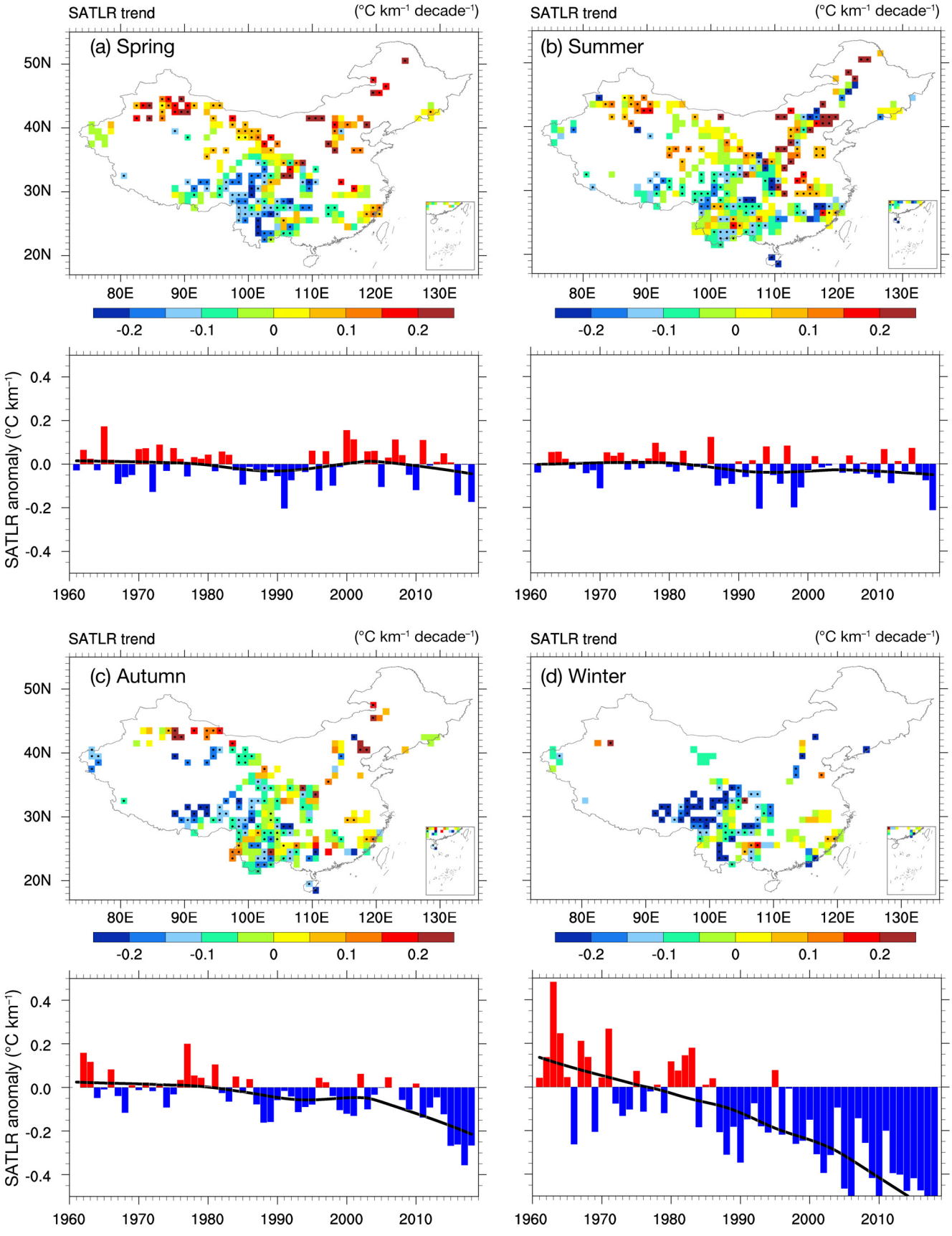

Fig. 7. Trend distribution of grid-box seasonal near-surface air temperature lapse rate (SATLR) anomalies and regional average seasonal SATLR anomalies in T_{min} for (a) spring, (b) summer, (c) autumn, and (d) winter. Other details as in Fig. 3

5. CONCLUSIONS

Regional average annual, autumn, and winter SATLR anomalies in T_{mean}, T_{max}, and T_{min} decreased significantly over 1961–2018, indicating that on the whole, the high altitudes warmed faster than the low altitudes in the mountainous areas of China's mainland. In terms of spatial distribution, both positive trends and negative trends of SATLR were found in all seasons, which revealed the inhomogeneity and complexity of warming across China's mainland. Most of the negative SATLR trends in T_{max} occurred in the central part of China, but in the southwestern part of China for T_{min}. Widespread negative SATLR trends were usually found in winter in T_{min}, especially in the Hengduan Mountains and the eastern part of the Tibetan Plateau. Widespread positive SATLR trends were observed in spring in T_{max}, mostly distributed in northern mountainous areas. The phenomenon might be caused by the difference of SATLR sensitivity between T_{max} and T_{min} to the variation of climatic variables, and the mechanism will be needed to be studied further in the future.

In the context of global and regional warming, the long-term trend of SATLR has the potential to be applied for detecting differences in the altitude response to climate warming on a small spatial scale, and for examining the local effect of EDW.

Acknowledgements. This work was supported by the Chinese Ministry of Science and Technology (MOST) National Key R&D Program (No. 2018YFA0605603). We thank Yunxin Huang, Tianlin Zhai, Huqiang Qin, and Kangmin Wen for their kind assistance.

LITERATURE CITED

Atabay D (2016) Pyrenn: first release, version 0.1. https://zenodo.org/records/45022

Blandford TR, Humes KS, Harshburger BJ, Moore BC, Walden VP, Ye H (2008) Seasonal and synoptic variations in near-surface air temperature lapse rates in a mountainous basin. J Appl Meteorol Climatol 47:249–261

Brunsdon C, Fotheringham AS, Charlton ME (1996) Geographically weighted regression: a method for exploring spatial nonstationarity. Geogr Anal 28:281–298

Cao L, Zhu Y, Tang G, Yuan F, Yan Z (2016) Climatic warming in China according to a homogenized data set from 2419 stations. Int J Climatol 36:4384–4392

Cleveland WS (1979) Robust locally weighted regression and smoothing scatterplots. J Am Stat Assoc 74:829–836

Du M, Zhang M, Wang S, Zhu X, Che Y (2018) Near-surface air temperature lapse rates in Xinjiang, northwestern China. Theor Appl Climatol 131:1221–1234

ESRI (2018) How GWR works. https://desktop.arcgis.com/en/arcmap/10.3/tools/spatial-statistics-toolbox/how-gwr-regression-works.htm

Fischer MM, Getis A (eds) (2010) Handbook of applied spatial analysis. Springer, Berlin

Fotheringham AS, Brunsdon C, Charlton M (2002) Geographically weighted regression: the analysis of spatially varying relationships. Wiley, Chichester

Gardner AS, Sharp MJ, Koerner RM, Labine C and others (2009) Near-surface temperature lapse rates over Arctic glaciers and their implications for temperature downscaling. J Clim 22:4281–4298

Guo X, Wang L, Tian L (2016) Spatio-temporal variability of vertical gradients of major meteorological observations around the Tibetan Plateau. Int J Climatol 36:1901–1916

Hartmann DL (2016) Global physical climatology, 2nd edn. Elsevier, Oxford

He Y, Wang K (2020) Contrast patterns and trends of lapse rates calculated from near-surface air and land surface temperatures in China from 1961 to 2014. Sci Bull 65:1217–1224

Hirsch RM, Slack JR, Smith RA (1982) Techniques of trend analysis for monthly water quality data. Water Resour Res 18:107–121

Jones PD, Hulme M (1996) Calculating regional climatic time series for temperature and precipitation: methods and illustrations. Int J Climatol 16:361–377

Kattel DB, Yao T, Yang K, Tian L, Yang G, Joswiak D (2013) Temperature lapse rate in complex mountain terrain on the southern slope of the central Himalayas. Theor Appl Climatol 113:671–682

Kattel DB, Yao T, Panday PK (2018) Near-surface air temperature lapse rate in a humid mountainous terrain on the southern slopes of the eastern Himalayas. Theor Appl Climatol 132:1129–1141

Kendall MG (1957) Rank correlation methods. Biometrika 44:298

Li X, Wang L, Chen D, Yang K, Xue B, Sun L (2013) Near-surface air temperature lapse rates in the mainland China during 1962–2011. J Geophys Res Atmos 118:7505–7515

Li Y, Zeng Z, Zhao L, Piao S (2015) Spatial patterns of climatological temperature lapse rate in mainland China: a multi-time scale investigation. J Geophys Res Atmos 120:2661–2675

Lu B, Brunsdon C, Charlton M, Harris P (2017) Geographically weighted regression with parameter-specific distance metrics. Int J Geogr Inf Sci 31:982–998

Mann HB (1945) Nonparametric tests against trend. Econometrica 13:245–259

Marshall SJ, Sharp MJ, Burgess DO, Anslow FS (2007) Near-surface-temperature lapse rates on the Prince of Wales Icefield, Ellesmere Island, Canada: implications for regional downscaling of temperature. Int J Climatol 27:385–398

Minder JR, Mote PW, Lundquist JD (2010) Surface temperature lapse rates over complex terrain: lessons from the Cascade Mountains. J Geophys Res Atmos 115:D14122

Mitchell A (2005) The ESRI guide to GIS analysis. ESRI Press, New York, NY

Mountain Research Initiative EDW Working Group (2015) Elevation-dependent warming in mountain regions of the world. Nat Clim Change 5:424–430

Ojha R (2017) Assessing seasonal variation of near surface air temperature lapse rate across India. Int J Climatol 37:3413–3426

Pepin N (2001) Lapse rate changes in northern England. Theor Appl Climatol 68:1–16

Pepin N, Kidd D (2006) Spatial temperature variation in the Eastern Pyrenees. Weather 61:300–310

Pepin NC, Lundquist JD (2008) Temperature trends at high elevations: patterns across the globe. Geophys Res Lett 35:L14701

Pepin NC, Seidel DJ (2005) A global comparison of surface and free-air temperatures at high elevations. J Geophys Res Atmos 110:D03104

Pepin N, Benham D, Taylor K (1999) Modeling lapse rates in the maritime uplands of Northern England: implications for climate change. Arct Antarct Alp Res 31:151–164

Qin Y, Ren G, Zhang P, Wu L, Wen K (2021a) An imputation method for the climatic data with strong seasonality and spatial correlation. Theor Appl Climatol 144:203–213

Qin Y, Ren G, Huang Y, Zhang P, Wen K (2021b) Application of geographically weighted regression model in the estimation of surface air temperature lapse rate. J Geogr Sci 31:389–402

Rolland C (2003) Spatial and seasonal variations of air temperature lapse rates in Alpine regions. J Clim 16:1032–1046

Sen PK (1968) Estimates of the regression coefficient based on Kendall's tau. J Am Stat Assoc 63:1379–1389

Shen YJ, Shen Y, Goetz J, Brenning A (2016) Spatial-temporal variation of near-surface temperature lapse rates over the Tianshan Mountains, central Asia. J Geophys Res Atmos 121:14006–14017

Tang Z, Fang J (2006) Temperature variation along the northern and southern slopes of Mt. Taibai, China. Agric For Meteorol 139:200–207

von Storch H, Navarra A (1999) Analysis of climate variability: applications of statistical techniques, 2nd edn. Springer, Berlin

Wang XL, Swail VR (2001) Changes of extreme wave heights in northern hemisphere oceans and related atmospheric circulation regimes. J Clim 14:2204–2221

Wang Q, Fan X, Wang M (2014) Recent warming amplification over high elevation regions across the globe. Clim Dyn 43:87–101

Wang Y, Wang L, Li X, Chen D (2018) Temporal and spatial changes in estimated near-surface air temperature lapse rates on Tibetan Plateau. Int J Climatol 38:2907–2921

Whiteman CD (2000) Mountain meteorology: fundamentals and applications. Oxford University Press, New York, NY

You Q, Kang S, Pepin N, Flügel WA, Yan Y, Behrawan H, Huang J (2010) Relationship between temperature trend magnitude, elevation and mean temperature in the Tibetan Plateau from homogenized surface stations and reanalysis data. Global Planet Change 71:124–133

Zhang X, Vincent LA, Hogg WD, Niitsoo A (2000) Temperature and precipitation trends in Canada during the 20th century. Atmos-Ocean 38:395–429

Editorial responsibility: Oliver Frauenfeld, College Station, Texas, USA
Reviewed by: D. B. Kattel and 2 anonymous referees

Submitted: December 28, 2022
Accepted: October 19, 2023
Proofs received from author(s): December 25, 2023